

Brain volumetric changes in the general population following the COVID-19 outbreak and lockdown

Tom Salomon¹, Adi Cohen^{1,2}, Gal Ben-Zvi^{1,2}, Rani Gera^{1,2,3}, Shiran Oren^{1,2}, Dana Roll¹, Gal Rozic¹, Anastasia Saliy¹, Niv Tik^{2,4}, Galia Tsarfati⁵, Ido Tavor^{*2,4,6}, Tom Schonberg^{*1,2,6}, Yaniv Assaf^{*1,2,6}

* corresponding authors equal contribution

1. School of Neurobiology, Biochemistry and Biophysics, Faculty of Life Science, Tel Aviv University, Tel Aviv, Israel
2. Sagol School of Neuroscience, Tel Aviv University, Tel Aviv, Israel
3. School of Psychological Sciences, Tel Aviv University, Tel Aviv, Israel
4. Department of Anatomy and Anthropology, Faculty of Medicine, Tel Aviv University, Tel Aviv, Israel
5. Division of Diagnostic Imaging, Sheba Medical Center, Tel-Hashomer, affiliated to the Faculty of Medicine, Tel Aviv University, Tel Aviv, Israel
6. The Strauss Center for Computational Neuroimaging, Tel Aviv University, Tel Aviv, Israel

Abstract

The COVID-19 outbreak introduced unprecedented health-risks, as well as pressure on the financial, social, and psychological well-being due to the response to the outbreak¹⁻⁴. Here, we examined the manifestations of the COVID-19 outbreak on the brain structure in the healthy population, following the initial phase of the pandemic in Israel. We pre-registered our hypothesis that the intense experience of the outbreak potentially induced stress-related brain modifications⁵⁻⁸. Volumetric changes in $n = 50$ participants scanned before and after the COVID-19 outbreak and lockdown, were compared with $n = 50$ control participants that were scanned twice prior to the pandemic. The pandemic provided a rare opportunity to examine brain plasticity in a natural experiment. We found volumetric increases in bilateral amygdalae, putamen, and the anterior temporal cortices. Changes in the amygdalae diminished as time elapsed from lockdown relief, suggesting that the intense experience associated with the pandemic outbreak induced volumetric changes in brain regions commonly associated with stress and anxiety⁹⁻¹¹.

Main text

Since early 2020, the world has been coping with the outbreak of the coronavirus disease 2019 (COVID-19) pandemic that has infected millions with devastating numbers of deaths globally. As an initial response to the first wave of the outbreak, countries closed their borders and implemented a series of ad-hoc laws and orders to restrict the spread of the disease. Countries with major outbreaks such as China, Italy, and Spain enforced stringent restriction of movement for a limited period, referred to here as ‘lockdown’. Although lockdowns contributed to restricting the health risks of the outbreak¹², they also had a negative impact on the social,

economic and psychological well-being of the general population, leading to one of the sharpest declines in economic growth over the past decades^{1,2}. Lockdowns also led to high rates of stress and anxiety which were attributed in large to the social and financial consequences of responding to the health crisis⁴. It is now evident that the indirect consequences of the pandemic affected a much larger proportion of the population, having an impact of no lesser gravity than the actual health risks that were meant to be prevented^{3,13}.

In Israel, a strict lockdown period was issued from mid-March until the end of April. During its peak, most unessential businesses were closed and civilians' movement for non-essential destinations was restricted for a radius of 100 meters from their homes. Prior to COVID-19, the country had experienced a period of peak economic prosperity¹⁴, which was interrupted by the outbreak, leading to unprecedented unemployment rates (reaching nearly 30% of the work-force in April 2020) and the collapse of several sectors such as aviation, tourism, and culture^{15,16}. The outbreak period was characterized with acute uncertainty and increase in anxiety, regarding both the health and socioeconomic effects of the pandemic¹⁷.

Over the past years several studies demonstrated brain plasticity detected using T1-weighted magnetic resonance imaging (MRI)¹⁸⁻²⁰. The current work was initiated as a reaction to the outbreak of COVID-19 in Israel, aimed to study the structural brain plasticity in the general population following a real-life event of global scale. For this purpose, we examined $n = 50$ test group participants that were scanned with T1-weighted MRI prior to the outbreak and returned for a follow-up scan after the lockdown period. The structural changes of the study group (before versus after the outbreak) were compared to those of $n = 50$ control participants who were scanned twice before the COVID-19 outbreak. The unique circumstances imposed due to the

COVID-19 lockdown created rare settings for a natural experiment to examine the effect of a real-world intense event on brain plasticity.

All participants were healthy, without a history of neurological or psychiatric disorders, did not show COVID-19 symptoms, and were not diagnosed carrying the virus (see the methods section for further demographic information). The hypotheses and general design of the current study were pre-registered prior to the completion of data collection and were based on a small independent pilot sample with $N = 16$ participants ($n = 8$ participants in each group). The data and analysis codes are openly shared online (project page: <https://osf.io/wu37z/>; preregistration: <https://osf.io/k6xhn/>).

Prior to their follow-up MRI scan session, we asked participants of the post-lockdown test group to fill in a short questionnaire regarding the lockdown period (see methods). Of the participants who agreed to reply, 79.6% reported they did not leave their home for non-essential needs, 38.8% indicated an increased feeling of anxiety following the lockdown, 79.6% met no more than 3 people, 34.7% anticipated that their future behavior will change after the lockdown, 44.9% did not meet with their parents at all, 42.9% indicated that their employment status was reduced to part-time or unemployment, 46.8% reported they were concerned about their personal future well-being. In an exploratory principal component analysis (PCA), we found that two principal components best explain the variability in the data, explaining together 42.58% of the variance. The first component was highly loaded with increased feelings of anxiety, and the second was related to items describing increased social isolation (Figure 1). These analyses (not included in the pre-registration) indicate that the pandemic outbreak had a significant impact on the social and psychological well-being of most participants in our study.

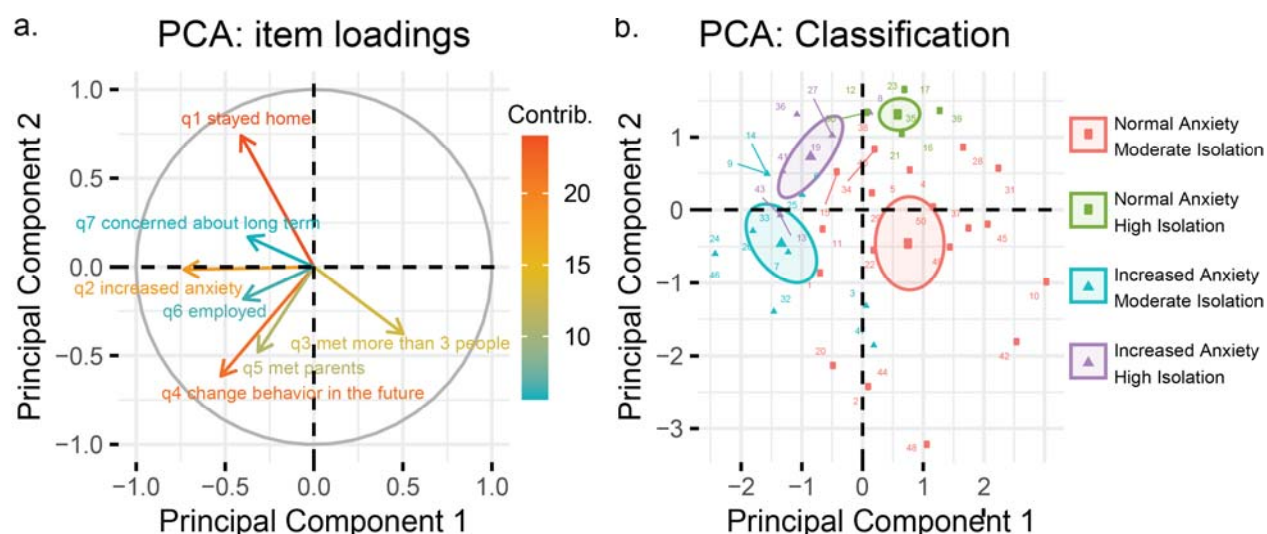


Figure 1. Principal component analysis of COVID-19 questionnaire.

A principal component analysis (PCA) of the responses to the questionnaire revealed two main themes characterized the participants. **a.** An increased feeling of anxiety dominated the first principal component (x-axis), while the three items relating to social distancing (staying at home, meeting parents and meeting more than 3 people) contributed together to the second component (y-axis). **b.** Visualization of participants dispersion across the two principal components and their categorization into binary anxiety and isolation groups. High isolation was defined as directional response to all three social-isolation items described above. Points represent individual participants.

Based on our pilot study results and previous studies of stress-related morphological brain changes⁵⁻⁸ we hypothesized that the focus of volumetric changes will be observed mainly in the amygdalae. The anatomical data were used as input for deformation and surface-based morphometry (SBM) analysis using the CAT12 toolbox (<http://www.neuro.uni-jena.de/cat/>, University of Jena) for SPM12 (<http://www.fil.ion.ucl.ac.uk/spm/software/spm12/>, Wellcome Trust Centre for Neuroimaging). The brain was segmented to 58 regions based on the cortical and subcortical nuclei classifications of the Hammers atlas (Hammers et al., 2003). Following surface reconstruction, each participant's individual gray matter volume was estimated for each of the 58 anatomically defined regions of interest (ROIs). This procedure accounted for the longitudinal nature of the data, performing the analysis on both scans simultaneously. To avoid voxel-based multiple comparisons, we performed a region-based analysis (following surface

projection to the Hammer atlas) and corrected for multiple comparisons using the Benjamini-Hochberg correction²¹ to control for false discovery rate (FDR; at $p < 0.05$ following correction). Validation of this pipeline was performed using simulated data and by comparing the results with other software (see methods).

Using a linear mixed model, we examined volumetric changes, testing for regions with stronger effects for the test group, compared to the control group. Examining an interaction effect of session (baseline versus follow-up scans) and experimental group (test versus control) revealed ten anatomical brain regions (composed of bilateral five unique regions in both hemispheres) in which volumetric increases were observed uniquely for the test group (Table 1 and Figure 2). Most prominently, as we expected and pre-registered, we found a robust effect in the bilateral amygdalae. We also observed a significant effect bilaterally in the putamen, and in three anatomical regions within the ventral anterior temporal cortex adjacent to each other, namely in the medial part of the anterior temporal lobe, the fusiform gyrus, and the parahippocampal gyrus. To examine the spatial distribution within significant ROIs, we performed an additional post-hoc voxel-based analysis, which allowed us to visualize the changes within the significant ROIs (Figure 2a). Examining the post-hoc voxel-based results revealed that volumetric changes occurred throughout the entire surface of bilateral amygdalae, while in the putamen the effects occurred mainly in the dorsal area. In the ventral anterior temporal cortices, large connected clusters of volumetric change spanned throughout the three adjacent temporal ROIs, thus suggesting that the three ROIs shared a similar origin. In all ROIs, we ensured that the significant effect was apparent for the test group but not for the control group (see methods), suggesting that the reported interaction effects originated from volumetric changes in the test group following the COVID-19 outbreak and its related lockdown period (Figure 2b).

Table 1. Surface based morphology analysis results

| Region | Hemi-sphere | Interaction estimate (95% CI) | Interaction <i>p</i> (FDR adj.) | Session estimate (95% CI) ^a | Session <i>p</i> (FDR adj.) |
|--------------------------------------|-------------|-------------------------------|---------------------------------|--|--|
| Amygdala | Left | 0.09 [0.05, 0.13] | 2.4E ⁻⁵ (0.001) | 0.08 [0.05, 0.11] | 9.8E ⁻⁶ (2.1E ⁻⁴) |
| | Right | 0.08 [0.03, 0.13] | 0.003 (0.030) | 0.08 [0.05, 0.11] | 1.6E ⁻⁵ (2.3E ⁻⁴) |
| Putamen | Left | 0.19 [0.09, 0.29] | 4.1E ⁻⁴ (0.006) | 0.13 [0.06, 0.2] | 4.0E ⁻⁴ (0.002) |
| | Right | 0.17 [0.08, 0.26] | 2.4E ⁻⁴ (0.005) | 0.14 [0.08, 0.2] | 1.1E ⁻⁵ (2.1E ⁻⁴) |
| Anterior temporal lobe (medial part) | Left | 0.25 [0.12, 0.38] | 1.8E ⁻⁴ (0.005) | 0.15 [0.07, 0.23] | 4.7E ⁻⁴ (0.003) |
| | Right | 0.21 [0.07, 0.35] | 0.004 (0.030) | 0.15 [0.05, 0.25] | 0.004 (0.023) |
| Parahippocampal gyrus | Left | 0.09 [0.03, 0.15] | 0.006 (0.035) | 0.04 [0, 0.08] | 0.029 (0.085) |
| | Right | 0.11 [0.04, 0.18] | 0.003 (0.030) | 0.08 [0.03, 0.13] | 0.002 (0.009) |
| Fusiform gyrus | Left | 0.08 [0.03, 0.13] | 0.007 (0.036) | 0.06 [0.03, 0.09] | 3.8E ⁻⁴ (0.003) |
| | Right | 0.11 [0.04, 0.18] | 0.002 (0.022) | 0.05 [0, 0.1] | 0.044 (0.111) |

^a Session estimate examined the effect of baseline versus follow-up scan in the post-lockdown test group. This parameter was used to validate that the interaction effect observed between the group stemmed from a robust effect in the test group (see methods).

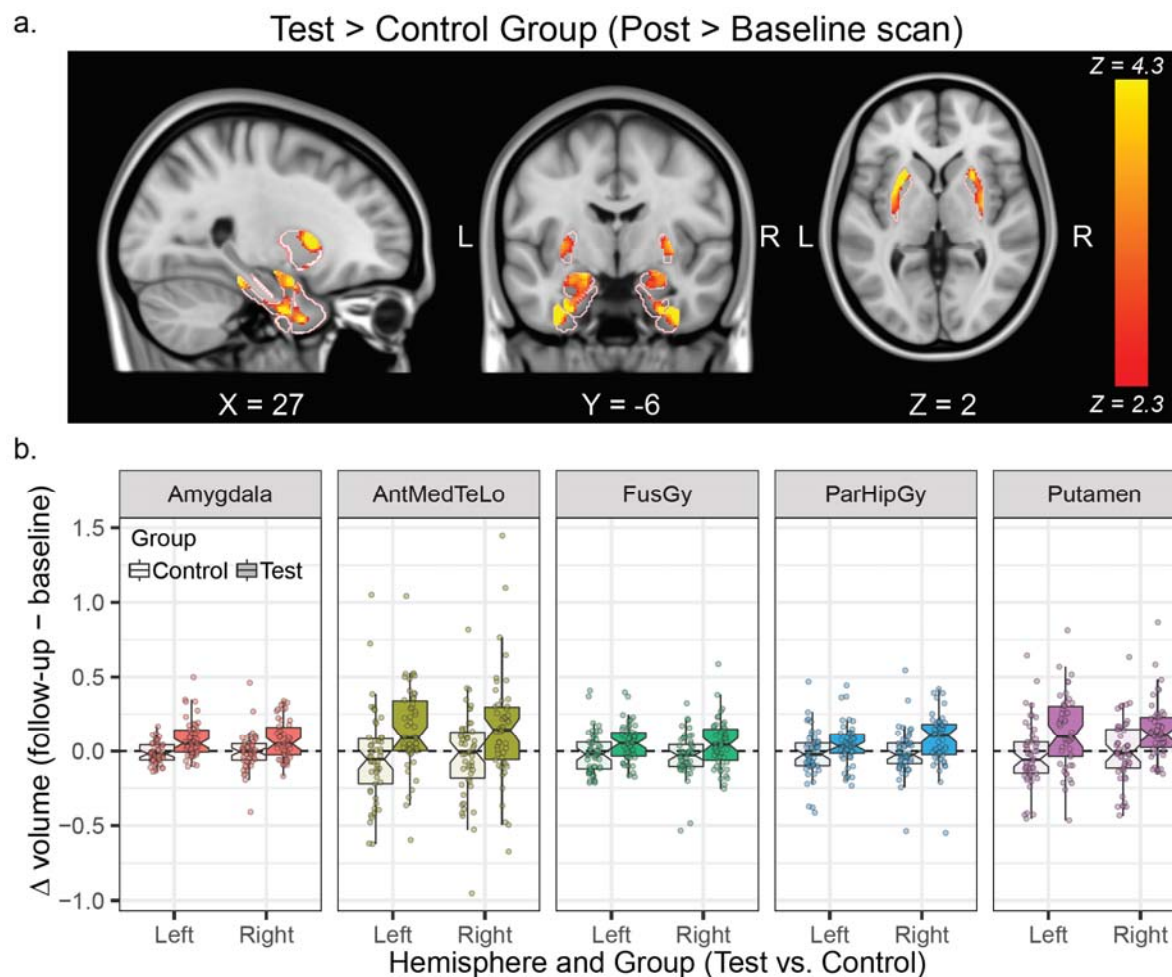


Figure 2. Volumetric changes results.

An interaction effect for time (baseline versus follow-up scan) and group (test versus control) was evaluated on segmented surfaces in an SBM analysis. Significant interaction effects were observed bilaterally in the amygdala and putamen ROIs, as well as in three ventral temporal cortical ROIs. **a.** To examine spatial patterns within the identified ROIs, a post-hoc voxel-based analysis was conducted within each ROI mask. Light red contours represent segmentation borders of the ROIs. **b.** Individual distribution of the results in the control group (light colors) and test group (dark colors). Box-plot center, hinges, and whiskers represent the median, quartiles, and from the hinges, respectively. A notch of represent an estimated 95% confidence interval for comparing medians. Dots represent individual participants. Abbreviated ROI names: AntMedTeLo = anterior temporal lobe (medial part); FusGy = fusiform gyrus, ParHipGy = Parahippocampal gyrus.

To evaluate and control for the effect of time between scans and time from lockdown, we included in the model two additional covariates - the time between scans (TBS; which was generally longer for the test group) and time following lockdown (TFL; see supplementary methods for more details). The two covariates were not correlated with each other in our test

group sample ($r = -0.106$, $t(48) = -0.74$, $p = 0.463$). Our reported regions demonstrated significant volumetric change above and beyond these covariates. After FDR correction, no region showed an effect of TBS. However, we did find a negative effect of TFL in the two amygdalae ROIs and the left fusiform gyrus, suggesting that the volumetric changes in these regions moderated as time following lockdown elapsed. Based on these results we estimated the time to decay as the estimated number of days from lockdown until volumetric changes returned to normal levels, similar to those of the control group (left amygdala: $\beta_{\text{TFL}} = -0.41$, $t(47) = -3.1$, $p = 0.003$, $p_{\text{adj.}} = 0.048$, time to decay = 95 days; right amygdala: $\beta_{\text{TFL}} = -0.54$, $t(47) = -4.38$, $p = 6.7\text{E}^{-5}$, $p_{\text{adj.}} = 0.002$, time to decay = 83 days; left fusiform gyrus: $\beta_{\text{TFL}} = -0.54$, $t(47) = -4.44$, $p = 5.5\text{E}^{-5}$, $p_{\text{adj.}} = 0.002$, time to decay = 82 days; Figure 3).

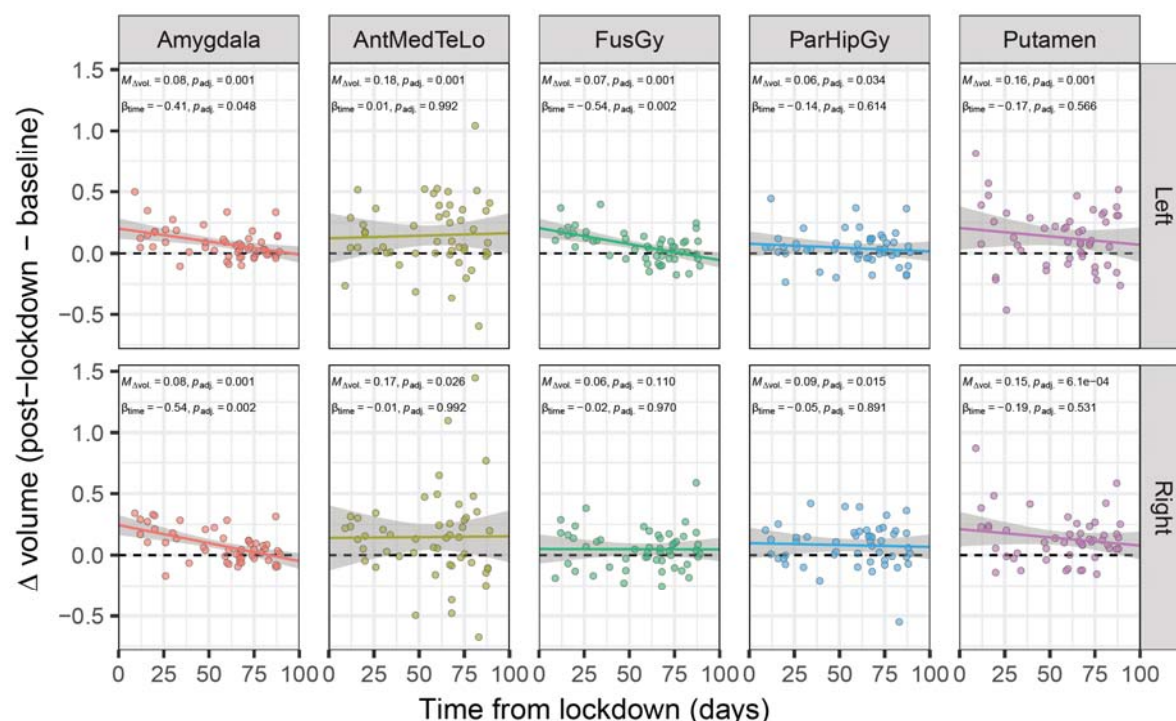


Figure 3. Time following lockdown effect on volumetric changes.

The time from lockdown relief until the follow-up scan session (TFL) was introduced as addition covariate to the model, revealing significant effect in the two amygdalae and left fusiform gyrus. Points represent individual participants in the post-lockdown test, p -values were FDR adjusted for multiple comparisons. Abbreviated ROIs: AntMedTeLo = anterior temporal lobe (medial part); FusGy = fusiform gyrus, ParHipGy = Parahippocampal gyrus.

Additional exploratory analyses examined the association of volumetric changes and the reported experience during lockdown. We found no strong association between the two, as reported in the supplementary results.

In conclusion, our study demonstrates that volumetric change patterns in the brain occurred following the COVID-19 initial outbreak period and restrictions. Previous studies demonstrated brain plasticity using T1-weighted MRI following planned interventions^{18–20}. The current work uniquely demonstrates stark structural brain plasticity following a major real-life event.

Our findings show changes in gray matter in the amygdala, putamen and ventral anterior temporal cortex. The changes in the amygdalae showed a temporal-dependent effect, related to the time elapsed from lockdown but not the duration from the baseline scan. It should be noted that although lockdown restrictions had initially reduced infection rates in Israel, just one month after the lockdown was lifted, the number of infected cases started to rise again and reached higher number of active infected cases by the end of data collection, compared with the peak numbers during the actual lockdown period (approximately 2,000 daily new cases by the end of July versus under 750 new daily cases during the peak of the lockdown period in April²², see supplementary Figure 1). This suggests that the effects observed in the current study are less likely to be attributed to the concrete health risks of COVID-19, but rather to the first wave of the outbreak, characterized with perceived uncertainty.

The current study was in many aspects unplanned; thus we are left with only partial answers as to which specific components of the COVID-19 outbreak led to the neural changes observed in the healthy participants that took part in our study. The involvement of the amygdala may suggest that stress and anxiety could be the source of the observed phenomenon, due to its well-recorded functional and structural associations^{5–11}. Nevertheless, it is hard to draw clear

conclusions as many aspects of life have changed in this time period, and could have potentially affected different regions in the brain – from limiting social interactions, increased financial stress, changes in physical activity, work routine, and many more. The limited behavioral data collected in the current study did not provide a strong connection to the imaging results, and thus future work could try to better address the complex brain-behavioral associations in this real-life experience. Nonetheless, our findings show healthy young adults, with no records of mental health issues, were deeply affected by the outbreak of COVID-19. We suggest that policy makers take into consideration the impact of their actions on the general well-being of the population they seek to help, alongside the efficacy of disease prevention.

Acknowledgements

This work was supported by the Israeli Science Foundation granted to Yaniv Assaf (ISF 1314/15), Tom Schonberg (2004/15), and Ido Tavor (ISF 1603/18). Tom Salomon was supported by the Nehemia Levtzion fellowship and the Fields-Rayant Minducate Learning Innovation Research Center. We would also want to thank Dr. Daniel Barazany, the manager of the Strauss MRI center, for his invaluable assistance throughout the study.

Author contributions

T.Sa. wrote the manuscript with Y.A, assisted with the study design and analyzed the data. Data was collected by A.C., R.G, S.O, G.R., D.R, and A.S. Free-surfer analysis was made by G.B-Z. N.T performed VBM validation analysis. G.T. provided support and medical supervision. I.T., T.Sc. and Y.A. conceived the study, wrote the manuscript and supervised the study. Y.A

performed the preprocessing and analysis of imaging data. All Author contributed intellectually and reviewed the manuscript.

Competing interests

The authors declare no competing financial interests.

References

1. Zhang, D., Hu, M. & Ji, Q. Financial markets under the global pandemic of COVID-19. *Financ. Res. Lett.* 101528 (2020). doi:10.1016/j.frl.2020.101528
2. Fernandes, N. Economic effects of coronavirus outbreak (COVID-19) on the world economy Nuno Fernandes Full Professor of Finance IESE Business School Spain. *SSRN Electron. Journal*, ISSN 1556-5068, Elsevier BV, 0–29 (2020).
3. Gruber, J. *et al.* Mental health and clinical psychological science in the time of COVID-19: Challenges, opportunities, and a call to action. *Am. Psychol.* (2020). doi:https://doi.org/10.1037/amp0000707
4. Taylor, S. *et al.* COVID stress syndrome: Concept, structure, and correlates. *Depress. Anxiety* 1–9 (2020). doi:10.1002/da.23071
5. Ganzel, B. L., Kim, P., Glover, G. H. & Temple, E. Resilience after 9/11: Multimodal neuroimaging evidence for stress-related change in the healthy adult brain. *Neuroimage* **40**, 788–795 (2008).
6. Hölzel, B. K. *et al.* Stress reduction correlates with structural changes in the amygdala. *Soc. Cogn. Affect. Neurosci.* **5**, 11–17 (2009).
7. Rogers, M. A. *et al.* Smaller amygdala volume and reduced anterior cingulate gray matter density associated with history of post-traumatic stress disorder. *Psychiatry Res. - Neuroimaging* **174**, 210–216 (2009).
8. Schienle, A., Ebner, F. & Schäfer, A. Localized gray matter volume abnormalities in generalized anxiety disorder. *Eur. Arch. Psychiatry Clin. Neurosci.* **261**, 303–307 (2011).
9. Stevens, J. S. *et al.* Amygdala Reactivity and Anterior Cingulate Habituation Predict Posttraumatic Stress Disorder Symptom Maintenance After Acute Civilian Trauma. *Biol.*

Psychiatry **81**, 1023–1029 (2017).

10. Bryant, R. A. *et al.* Enhanced amygdala and medial prefrontal activation during nonconscious processing of fear in posttraumatic stress disorder: An fMRI study. *Hum. Brain Mapp.* **29**, 517–523 (2008).
11. Mochcovitch, M. D., Da Rocha Freire, R. C., Garcia, R. F. & Nardi, A. E. A systematic review of fMRI studies in generalized anxiety disorder: Evaluating its neural and cognitive basis. *J. Affect. Disord.* **167**, 336–342 (2014).
12. Vinceti, M. *et al.* Lockdown timing and efficacy in controlling COVID-19 using mobile phone tracking. *EClinicalMedicine* (2020). doi:10.1016/j.eclinm.2020.100457
13. Qiu, J. *et al.* A nationwide survey of psychological distress among Chinese people in the COVID-19 epidemic: Implications and policy recommendations. *Gen. Psychiatry* **33**, 1–4 (2020).
14. Bank of Israel Research Department. The Decline in Unemployment in Israel by International Comparison. in *Bank of Israel Annual Report 2019* (2020).
15. Bank of Israel Research Department. *The unemployment rate and its definition during the corona period.* (2020).
16. Bank of Israel Research Department. *Changes in credit card purchases as a result of the corona crisis.* (2020).
17. Tzur Bitan, D. *et al.* Fear of COVID-19 scale: Psychometric characteristics, reliability and validity in the Israeli population. *Psychiatry Res.* **289**, 113100 (2020).
18. Maguire, E. A. *et al.* Navigation-related structural change in the hippocampi of taxi drivers. *Proc. Natl. Acad. Sci. U. S. A.* **97**, 4398–4403 (2000).
19. Jung, W. H. *et al.* Exploring the brains of Baduk (Go) experts: Gray matter morphometry, resting-state functional connectivity, and graph theoretical analysis. *Front. Hum. Neurosci.* **7**, 633 (2013).
20. Draganski, B. *et al.* Changes in grey matter induced by training. *Nature* **427**, 311–312 (2004).
21. Benjamini, Y. & Hochberg, Y. Controlling the False Discovery Rate: A Practical and Powerful Approach to Multiple Testing. *J. R. Stat. Soc. Ser. B* **57**, 289–300 (1995).
22. Israel Ministry of Health. Coronavirus in israel - Overview (in Hebrew). (2020). Available at: <https://datadashboard.health.gov.il/>. (Accessed: 31st August 2020)

23. Champely, S. *et al.* Package ‘pwr’: Basic Functions for Power Analysis. *CRAN Repos.* (2018).
24. Manjón, J. V., Coupé, P., Martí-Bonmatí, L., Collins, D. L. & Robles, M. Adaptive non-local means denoising of MR images with spatially varying noise levels. *J. Magn. Reson. Imaging* **31**, 192–203 (2010).
25. Dahnke, R., Yotter, R. A. & Gaser, C. Cortical thickness and central surface estimation. *Neuroimage* **65**, 336–348 (2013).
26. Kassambara, A. & Mundt, F. factoextra: Extract and Visualize the Results of Multivariate Data Analyses. R package version 1.0.7 (2020). Available at: <https://cran.r-project.org/package=factoextra>.

Supplementary Methods

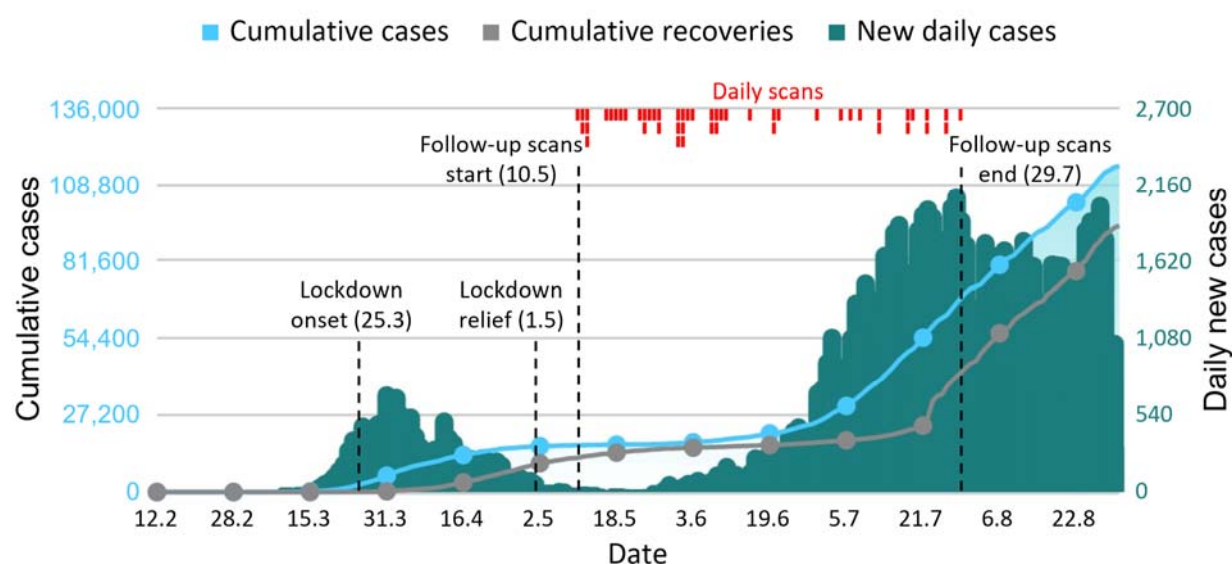
Codes and Data Accessibility

Our sample size, hypotheses and analyses plan were pre-registered on the Open Science Framework (OSF), soon after data collection began, but prior to completion of the data collection and data analysis (project page: <https://osf.io/wu37z/>; preregistration: <https://osf.io/k6xhn>). All behavioral processed imaging data along with the analysis codes are shared on the OSF project page. Uncorrected and small-volume corrected statistical maps of the voxel-based results described in the current work are available at <https://neurovault.org/collections/8591/>.

Participants

The study included two groups: A test group scanned before and after COVID-19 lockdown, and a control group, scanned twice before COVID-19 lockdown. All participants had no background of neurological disorders, did not show symptoms for COVID-19 and were not diagnosed as carriers of the virus. The study was approved by the ethics committee of Tel Aviv University and institutional review board (IRB) at the Sheba Tel-Hashomer medical center. Since the IRB protocol allowed us to scan the participants several times over a long period of time, we were able to collect the data from participants who were scanned prior to COVID-19 outbreak and invite them back for a follow-up scan as part of the longitudinal study they have agreed to take part in. Participants received monetary compensation for their time and gave their informed consent to take part in a longitudinal experiment aimed to examine brain plasticity across several sessions, which was initially not directly related to COVID-19 outbreak.

The test group comprised of $n = 50$ participants who were scanned before and after COVID-19 lockdown (Δ Time between scans: $M = 309.3$, $SD = 207.5$, range = 67 - 1460 days; Age: $M = 30.1$, $SD = 6.65$, range = 21 - 48; Females: $n = 20$, prop. = 40%). The lockdown period began on March 25th, and was gradually relieved throughout late April. We mark here May 1st as the lockdown relief date, as on this day an issued 100-meters movement limit for non-essential needs was lifted. The test group data collection started as soon as lockdown relief took place, for a period of approximately 3 months, until the end of July, 2020 (Δ Time from lockdown relief: $M = 57$, $SD = 24.62$, range = 9 - 89 days; see Supplementary figure 1 for the study timeline).



Supplementary Figure 1. Study timeline and outbreak data

On February 21st, 2020, the first COVID-19 case in Israel was recorded. Daily new cases are presented on green bars (right y-axis), along with the cumulative number of cases and recoveries (left y-axis). Data was retrieved and modified based on the Israeli Ministry of Health reports²². A lockdown was issued on March 25th, which was gradually released until the removal of the 100-meter restriction on May 1st, marking lockdown onset and relief, respectively (shorter vertical dashed line). MRI data of the test group was collected from May 10th to July 29th (longer vertical dashed line). Red bars on top represent the number of participants scanned for the study each day.

As a control group, we used the data of $n = 50$ participants who were scanned twice using a similar protocol before COVID-19 lockdown (Δ Time between scans: $M = 126.7$, $SD = 190.4$, range = 21 - 886 days; Age: $M = 27.3$, $SD = 5.63$, range = 19 - 42; Females: $n = 23$, prop. = 46%).

The minimal sample size was determined and pre-registered (<https://osf.io/uktsn>), based on a 80% power analysis conducted using R ‘pwr’ package²³, on a pilot study with $N = 16$ participants ($n = 8$ in each group). We decided to collect a minimum of $n = 37$ participants which should provide 80% to detect the group and session interaction effect with $\alpha = .05$, within both the left and right Amygdala. We originally committed to collect $n = 37$ participants in each group, under the assumption it would be difficult to complete the sample due to COVID-19 limitations. Eventually, thanks to further relief in COVID-19 restrictions, we were able to extend the sample size to $n = 50$ in each group.

The results remain generally consistent, even when the data included only the first $n = 37$ participant; demonstrating significant effects in the bilateral amygdalae, putamen, parahippocampal gyrus and the left anterior temporal lobe. In this smaller sample, we did not find significant effects in the right anterior temporal lobe, nor in the fusiform gyrus. We also found volumetric increase effects that were not identified using the full sample in the left nucleus accumbens, left cuneus, and left insula.

Imaging data

Acquisition protocol. Imaging data were acquired using a 3T Siemens Prisma scanner, with a 64-channel head coil. For the structural data, T1w high resolution (1-mm^3) whole brain images were acquired with a magnetization prepared rapid gradient echo (MPRAGE) pulse sequence with repetition time (TR) of 2.53s, echo time (TE) of 2.88ms, flip angle (FA) = 7° , field-of-view (FOV) = $224 \times 224 \times 208$ mm, resolution = $1 \times 1 \times 1$. (see below).

Some participants were also scanned with diffusion-weighted echo-planar imaging (DW EPI) sequence and some with functional gradient-echo EPI (GE EPI) in a resting state scan. The analyses of these scans are beyond the scope of the current study.

Data processing and analysis. The T1w MPRAGE anatomical scans were used for a surface-based morphometry (SBM) analysis. From the images we estimated the pial and inner surfaces of the cortex and projected those into the Hammers atlas (Hammers et al., 2003). Data were preprocessed in SPM12 (<http://www.fil.ion.ucl.ac.uk/spm/software/spm12/>, Wellcome Trust Centre for Neuroimaging) and SPM based CAT12 (Computational Anatomy Toolbox 12; <http://www.neuro.uni-jena.de/cat/>, University of Jena) extension. We deployed the CAT12 surface-processing pipeline, which includes skull stripping, a denoising filter²⁴ projection-based thickness estimation²⁵, partial volume correction, and spatial normalization to MNI space.

Surface-based volumetric data of cortical and subcortical regions were segmented based on the Hammers Atlas, segmenting the volumetric data into 58 anatomically defined regions. Ten additional ROIs of non-gray matter (ventricles, white matter, brain-stem and cerebellum ROIs) were excluded from statistical analyses. To evaluate the effect of lockdown on volumetric imaging data we ran a mixed linear model on the data within each one of the 58 anatomical regions, examining the effect of session (baseline versus follow-up scan) and group interaction (test versus control), controlling for time between scans (TBS) and time following lockdown (TFL) covariates. Both covariates were mean centered before they were added to the model.

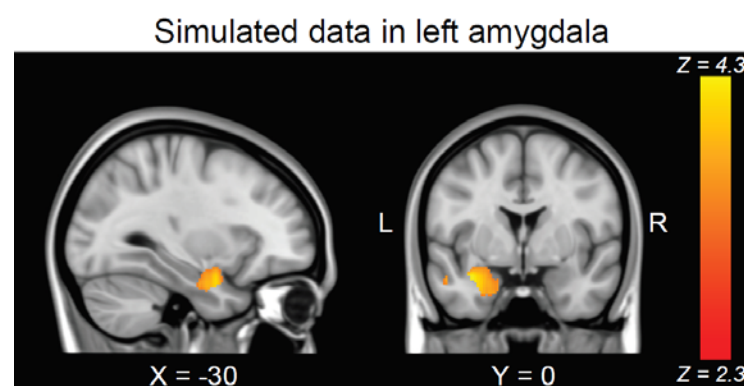
To identify our regions of interest we included only regions that showed both a significant interaction effect (i.e. the volumetric difference between the two sessions was significantly different for the test and control group), and a significant session effect within the test group (i.e. a significant difference between the two sessions for the test group). Results were corrected for multiple comparisons using the false discovery rate (FDR) correction, based on the number of brain regions tested²¹. Following the analysis pipeline, we identified ten significant ROIs: bilateral amygdalae, putamen, parahippocampal gyrus, the medial part of the anterior temporal lobe, and the fusiform gyrus.

An additional ROI of the right inferior and middle temporal gyri showed a significant interaction effect (interaction estimate = 0.17, 95% CI = [0.05, 0.29], $p = 6.1E^{-3}$, $p_{adj.} = 0.035$), however examining the test group separately, we could not identify a significant session effect (session estimate = 0.04, 95% CI = [-0.02, 0.10], $p = 0.259$, $p_{adj.} = 0.424$). Therefore, it is harder to interpret that this interaction effect stemmed from the test group. Thus, we did not include this ROI as one of our significant ROIs. A less robust session effect within the test group was also observed for the left parahippocampal gyrus (session estimate = 0.04 [0.00, 0.08], $p = 0.029$, $p_{adj.} = 0.085$) and right fusiform gyrus ROI (session estimate = 0.05 [0.00, 0.10], $p = 0.044$, $p_{adj.} = 0.111$), however as these ROIs demonstrated strong interaction effects and their session effects were significant before FDR correction, we decided to report them together with the other significant regions. A similar procedure was used in the pre-registration (i.e. including only regions that showed a significant interaction and an effect in the test group), however in the analysis of the pilot for the pre-registration, we used uncorrected results due to the small sample size.

To examine the spatial distribution of our effect within significant ROIs, that were identified with the SBM analysis, we performed an additional post-hoc voxel-based analysis. We projected the data on a voxel-based map, effectively examining which voxels demonstrated an interaction effect. Then, we used anatomical masks of ROIs which were found to be significant in the SBM analysis, to visualize the results within these regions, similarly to a small-volume correction analysis (Figure 2a)

Pipeline validation

To validate the imaging processing protocol we used two approaches, before data collection was completed (at the time of the pre-registration finalization). As many surface-based software focus on analysis of cortical surfaces, rather than subcortical regions, we aimed to validate that our SBM protocol using CAT12 could reliably identify subcortical morphological changes, such as the ones we observed in the current study within the amygdala and putamen. To test the detection capabilities of our protocol, we generated simulated data with volumetric changes in the amygdala and ran the pipeline on the simulated data. A volumetric increase in the amygdala was simulated using a hand-drawn polygon mask, surrounding the left amygdala on the original T1w images. Within this polygon 3D mask, the signal intensity was artificially changed. Following this procedure, both the original and modified T1w images underwent the same CAT12 pipeline. The analysis was performed on 10 participants. We were able to identify the simulated volumetric changes within the subcortical amygdala nuclei (see supplementary Figure 2).



Supplementary figure 2. Data simulation

Sub-cortical changes in the left amygdala were simulated in ten participants. The SBM pipeline applied in CAT12 identified the simulated change effect. Data was projected from surfaces back to a voxel-based map for visualization in the current figure.

In an additional validation procedure, we reanalyzed our results with an additional analysis pipeline. Raw T1-weighted maps were preprocessed using FreeSurfer. Using this alternative analysis pipeline, we found similar results, including robust effects on the temporal cortical regions in addition to other cortical regions. It should be noted that the FreeSurfer pipeline analyze only cortical surface, thus the analysis did not include subcortical regions of the amygdala and putamen.

The results of both validations indicated our analysis pipeline could reliably identify regional volumetric estimations. Using CAT12 provided an advantage by performing a longitudinal analysis of subcortical regions, including the amygdala which was pre-hypothesized and of great importance in the current work.

Behavioral data

Data collection. To evaluate participants' experience in the peak days of the COVID-19 outbreak, we asked them to fill out a 7-items questionnaire regarding their experience of the COVID-19 lockdown (see supplementary Table 1 for a description of the items). The questionnaires were filled out soon after the initiation of the study, when the lockdown's stringent 100-meters limitation was lifted. Most participants filled out the questionnaire on the day of the post-lockdown scan session, some filled it a few days before their second scanning session. A total of $n = 77$ participants filled out the COVID-19 questionnaire and comprised the potential pool of test group participants for the current study, out of which $n = 50$ were sampled and scanned. One participant was scanned but did not complete the questionnaire, therefore this participant's behavioral data were not used and analyses of the questionnaire were based on $n = 49$ valid participants.

Supplementary Table 1. COVID-19 lockdown questionnaire

| Question | Possible Answers (prop.) | Binary outcome (prop.) |
|--|--|--|
| 1. Did you stay home during the lockdown, except for essential needs / did not leave at all? | 0 - no 1 - yes | 0 - no (20.4%) 1 - yes (79.6%) |
| 2. Did the lockdown increase your feeling of anxiety? | 0 - no 1 - yes | 0 - no (61.2%) 1 - yes (39.8%) |
| 3. With how many people did you meet during the lockdown (including people you are living with at home)? | 0 - none 1 - up to three people 2 - up to five people 3 - up to ten people | 0 - up to three (79.6%) 1 - more (20.4%) |
| 4. Do you think your behavior will change following the lockdown? | 0 - no 1 - yes | 0 - no (65.3%) 1 - yes (34.7%) |
| 5. How did your meeting with your parents' routine look like during the lockdown? | 0 - same as before the lockdown 1 - with precaution measurements: distancing, mask, etc. 2 - did not visit at all | 0 - as before or with precautions (44.9%) 1 - did not visit (55.1%) |
| 6. What was your employment status during the lockdown? | 0 - same as before lockdown 1 - full time working from home 2 - part time working from home 3 - Furlough / unemployed | 0 - unemployed / part time (42.9%) 1 - same as before / full time from home (57.1%) |
| 7. How concerned are you with the long-term effect of the lockdown, regarding yourself? | 1 - 5 scale | 0 - low, score 1-2 (53.1%) 1 - moderate-high, score 3-5 (46.9%) |

Data analysis. Responses to the lockdown questionnaire were coded into binary responses, based on the sample median, splitting the sample into relatively similar sized groups for each item. To identify the main themes in the questionnaire which could be correlated with the imaging data, we performed a PCA analysis on the binarized data, using the “factoextra” R package²⁶. We found two principal components, which explained 42.6% of the variance in the sample data. These two components were extracted and correlated with the change in gray matter volumetric data in our regions of interest.

Supplementary results

As an exploratory analysis, we examined whether the volumetric brain changes were associated with the psychological constructs identified in our PCA analysis, based on participants' self-reports. We used two linear models aimed to explain the variability in each of the principal components, using the volumetric changes as our model features. Overall neither one of the two PCs were well associated with the volumetric changes (Principal component 1 model: $R^2 = 0.205$, $F(10,38) = 0.98$, $p = 0.475$; Principal component 2 model: $R^2 = 0.33$, $F(10,38) = 1.89$, $p = 0.077$).

While we did find some sporadic ROIs showing significant contribution within the models (measured as the significance of the ROI's β estimates), after FDR correction by the number of features in the model, none of the ROIs demonstrated a significant association with the PCs ($p_{adj.} > 0.05$).

Finally, we examined correlation patterns of the volumetric change for all brain regions aiming to identify shared change patterns across multiple ROIs. Hierarchical clustering of the correlation matrices revealed different patterns between the two groups (Supplementary figure 3). In the test group, three principal groups of clusters could be identified - the first included the palladium, hippocampus, amygdala, putamen, insula (all bilaterally), and right anterior cingulate cortex, the second cluster included mostly occipito-temporal cortical and subcortical nuclei, and the third included highly correlated regions of the frontal, parietal and occipital cortices. All regions that passed the statistical threshold of the SBM analysis (Table 1), except for the left fusiform gyrus, were grouped closely together within the first two clusters, and showed low to negative correlations the ROIs of the third cluster. This analysis could suggest that the origin of the volumetric change observed in the regions of the two clusters might be different. The regions that appear in cluster 1 are often reported in the studies that explore brain changes following stress, anxiety or traumatic events⁵⁻⁸, while the regions of the second cluster are less associated with specific phenomena.

A different pattern was observed in the control group, where the correlation pattern demonstrated stronger volumetric synchrony, (Supplementary figure 3b). This could suggest that changes in the control group were much more affected by within-participant effects, rather than an exogenous effect (which could be the outbreak and lockdown in the test-group). It is important to note in this context that in addition to the experience of the lockdown, the participants in the test group also had longer time gaps between the two scanning sessions, which might provide an

